Atrial extrasystoles enhance low-voltage fractionation electrograms in patients with atrial fibrillation

van Schie, Mathijs S.; Liao, Rongheng; Ramdat Misier, Nawin L.; Knops, Paul; Heida, Annejet; Taverne, Yannick J.H.J.; de Groot, Natasja M.S.

DOI
10.1093/europace/euad223

Publication date
2023

Document Version
Final published version

Published in
Europace : European pacing, arrhythmias, and cardiac electrophysiology : journal of the working groups on cardiac pacing, arrhythmias, and cardiac cellular electrophysiology of the European Society of Cardiology

Citation (APA)
van Schie, M. S., Liao, R., Ramdat Misier, N. L., Knops, P., Heida, A., Taverne, Y. J. H. J., & de Groot, N. M. S. (2023). Atrial extrasystoles enhance low-voltage fractionation electrograms in patients with atrial fibrillation. *Europace : European pacing, arrhythmias, and cardiac electrophysiology : journal of the working groups on cardiac pacing, arrhythmias, and cardiac cellular electrophysiology of the European Society of Cardiology*, *25*(9). https://doi.org/10.1093/europace/euad223

ESC European Society of Cardiology

Europace (2023) **25**, 1–9
https://doi.org/10.1093/europace/euad223

TRANSLATIONAL RESEARCH

Atrial extrasystoles enhance low-voltage fractionation electrograms in patients with atrial fibrillation

Mathijs S. van Schie [1], Rongheng Liao [1], Nawin L. Ramdat Misier [1], Paul Knops[1], Annejet Heida[1], Yannick J.H.J. Taverne[2], and Natasja M.S. de Groot [1,3]*

[1]Department of Cardiology, Erasmus Medical Center, Dr. Molewaterplein 40, 3015GD Rotterdam, the Netherlands; [2]Department of Cardiothoracic Surgery, Erasmus Medical Center, Rotterdam, the Netherlands; and [3]Department of Microelectronics, Signal Processing Systems, Faculty of Electrical Engineering, Mathematics and Computer Sciences, Delft University of Technology, Mekelweg 4, 2628CD Delft, the Netherlands

Received 2 May 2023; accepted after revision 14 July 2023; online publish-ahead-of-print 21 July 2023

Background and aims Atrial extrasystoles (AES) provoke conduction disorders and may trigger episodes of atrial fibrillation (AF). However, the direction- and rate-dependency of electrophysiological tissue properties on epicardial unipolar electrogram (EGM) morphology is unknown. Therefore, this study examined the impact of spontaneous AES on potential amplitude, -fractionation, -duration, and low-voltage areas (LVAs), and correlated these differences with various degrees of prematurity and aberrancy.

Methods and results Intra-operative high-resolution epicardial mapping of the right and left atrium, Bachmann's Bundle, and pulmonary vein area was performed during sinus rhythm (SR) in 287 patients (60 with AF). AES were categorized according to their prematurity index (>25% shortening) and degree of aberrancy (none, mild/opposite, moderate and severe). In total, 837 unique AES (457 premature; 58 mild/opposite, 355 moderate, and 154 severe aberrant) were included. The average prematurity index was 28% [12–45]. Comparing SR and AES, average voltage decreased (−1.1 [−1.2, −0.9] mV, $P < 0.001$) at all atrial regions, whereas the amount of LVAs and fractionation increased (respectively, +3.4 [2.7, 4.1] % and +3.2 [2.6, 3.7] %, $P < 0.001$). Only weak or moderate correlations were found between EGM morphology parameters and prematurity indices ($R^2 < 0.299$, $P < 0.001$). All parameters were, however, most severely affected by either mild/opposite or severely aberrant AES, in which the effect was more pronounced in AF patients. Also, there were considerable regional differences in effects provoked by AES.

Conclusion Unipolar EGM characteristics during spontaneous AES are mainly directional-dependent and not rate-dependent. AF patients have more direction-dependent conduction disorders, indicating enhanced non-uniform anisotropy that is uncovered by spontaneous AES.

* Corresponding author. Tel: +31 10 7035018. *E-mail address*: n.m.s.degroot@erasmusmc.nl

Graphical Abstract

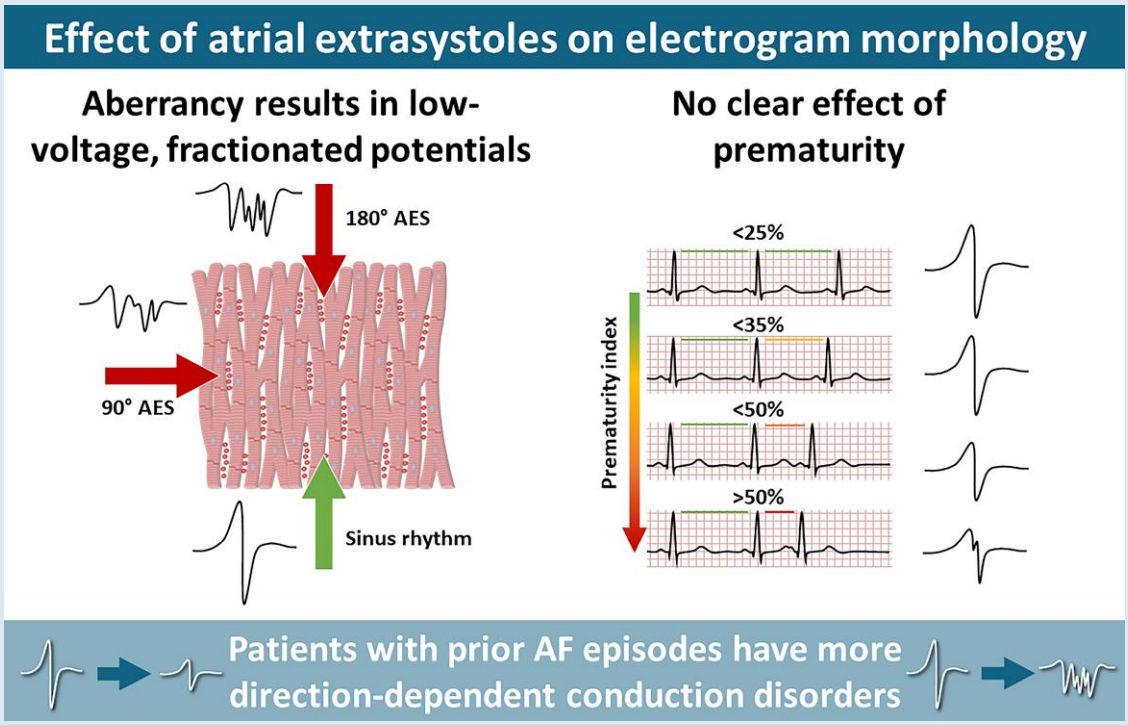

Keywords Atrial fibrillation • Sinus rhythm • Atrial extrasystole • High-resolution epicardial mapping • Anisotropy • Unipolar voltage • Potential morphology • Fractionation • Low-voltage areas • Conduction disorders

What's new?

- Unipolar electrogram characteristics during spontaneous atrial extrasystoles are mainly directional-dependent and not rate-dependent.
- Atrial extrasystoles with an opposite or perpendicular wavefront direction to sinus rhythm cause the largest decrease in potential voltages and increase in fractionation.
- Patients with atrial fibrillation have more direction-dependent conduction disorders particularly at the right atrium, indicating enhanced non-uniform anisotropy that is uncovered by spontaneous atrial extrasystoles.
- Enhanced non-uniform anisotropy present in patients with atrial fibrillation probably explains the higher vulnerability to trigger episodes of atrial fibrillation.

Introduction

Non-remodeled atrial tissue is considered to be anisotropic, resulting in a much faster electrical conduction along the longitudinal direction of myocardial fibers than in transverse direction.[1] Altered cell-to-cell communication and tissue damage results in a discontinuous distribution of conduction properties, which is known as non-uniform anisotropy. The presence of non-uniform anisotropy results in local conduction disorders and heterogeneous conduction, leading to increased susceptibility to tachyarrhythmias such as atrial fibrillation (AF).[2]

Atrial extrasystoles (AES) are common interruptions of sinus rhythm (SR), which may trigger episodes of AF. AES triggering AF most often originate from within the pulmonary veins (PV), especially in patients with paroxysmal AF.[3] However, non-PV triggers, emerging from, e.g. the superior vena cava, left atrial (LA) posterior free wall, LA appendage, terminal crest, and interatrial septum, also play an important role in a significant part of AF patients.[4] Especially in non-uniform anisotropic tissue, conduction disorders are direction and frequency dependent. Extracellular potentials recorded in these areas may be fractionated. This could be caused by asynchronous activation of two or more groups of cardiomyocytes that are separated by areas in which there is diminished or no cell-to-cell coupling.[5] The morphology of extracellular unipolar potentials can therefore be used to detect non-uniform anisotropic tissue.[6] High-resolution mapping during AES provides the opportunity to detect areas of direction and frequency dependent non-uniform anisotropy. The goal of this study was therefore to examine the impact of spontaneous AES on unipolar potential morphology and to correlate these differences with various degrees of prematurity and aberrancy in patients with and without history of AF.

Methods

Study population

The study population consisted of 287 successive adult patients with or without a history of AF undergoing open heart coronary artery bypass grafting (CABG), aortic or mitral valve surgery or a combination of valvular surgery and CABG in the Erasmus Medical Center Rotterdam. This study was approved by the institutional medical ethical committee (MEC2010-054/MEC2014-393).[7,8] Written informed consent was obtained from all patients. Patient characteristics (e.g. age, medical history, cardiovascular risk factors, time in AF) were obtained from the patient's medical record.

Mapping procedure

Epicardial high-resolution mapping was performed prior to commencement to extra-corporal circulation, as previously described in detail.[9] Epicardial mapping was performed with a 128-electrode array or 192-electrode array (electrode diameter, respectively, 0.65 or 0.45 mm, interelectrode distances 2.0 mm). Mapping was conducted by shifting the electrode array along imaginary lines with a fixed anatomic orientation, following a predefined mapping scheme, covering the entire epicardial surface of the right atrium (RA), Bachmann's Bundle (BB), pulmonary vein area (PVA) and left atrium (LA), as illustrated in *Figure 1*.

Five seconds of SR were recorded from every mapping site, including a surface ECG lead, a calibration signal of 2 mV and 1000 ms, a bipolar atrial reference electrogram (EGM) and all unipolar epicardial EGMs. In patients who presented in AF, SR mapping was performed after electrical cardioversion. Data were stored on a hard disk after amplification (gain 1000), filtering (bandwidth 0.5–400 Hz), sampling (1 kHz), and analogue to digital conversion (16 bits).

Data analysis

Unipolar EGMs were semi-automatically analyzed using custom-made software. The steepest negative slope of an atrial potential was marked as the local activation time (LAT). All annotations were manually checked with a consensus of two investigators. Several electrophysiological parameters

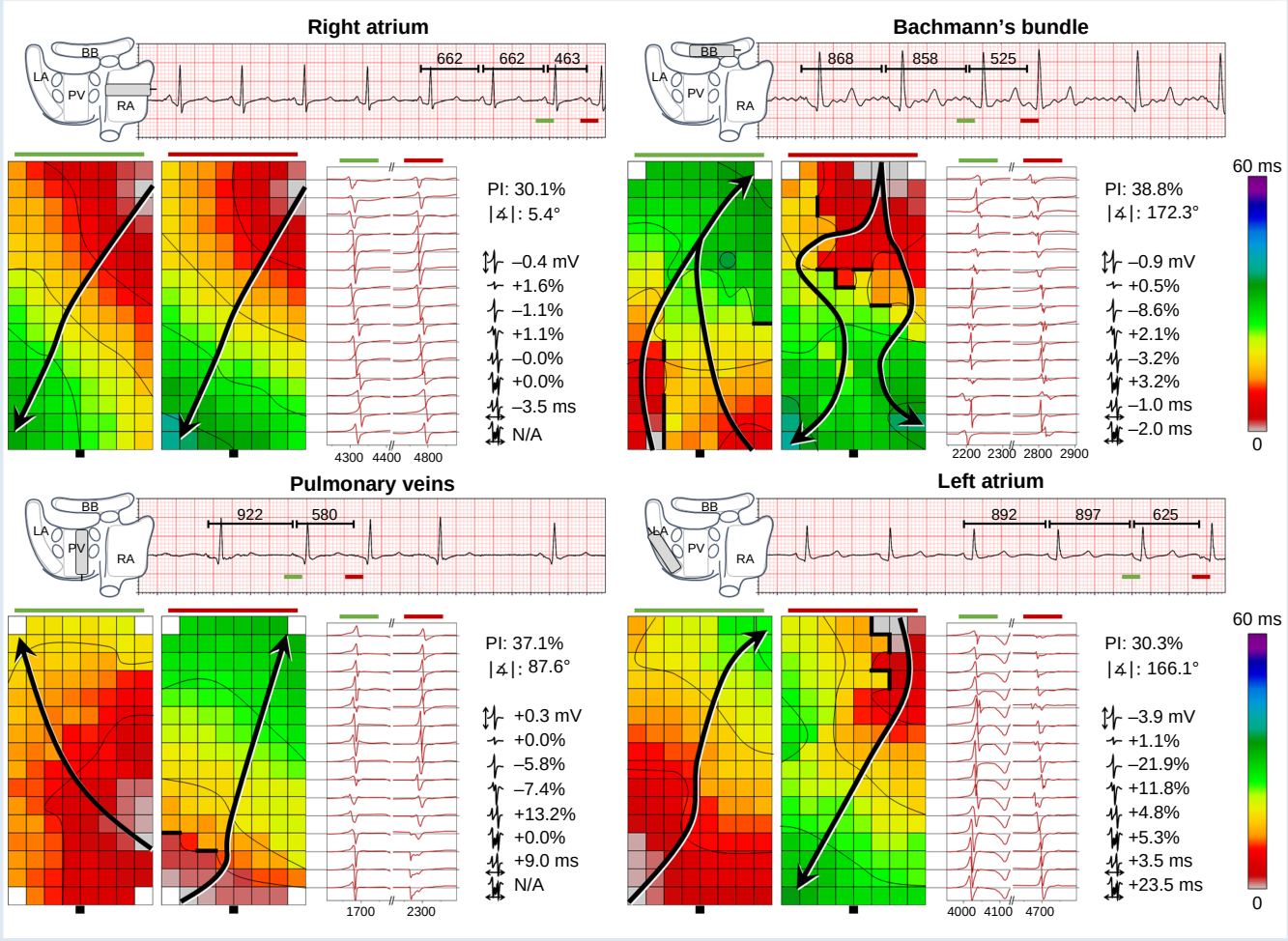

Figure 1 Examples of SR beats and AES recorded at various atrial sites. Four examples of 5 s SR recordings including AES and corresponding colour-coded activation maps and EGMs. Thick black lines in the activation maps correspond with conduction block according to a time difference between adjacent electrodes of ≥12 ms. For each patient, the PI, and average difference in wavefront direction, potential voltage, LVAs, amount of SP, SDP, LDP, and FP and their corresponding FD is given. Upper left panel: One SR beat and a mild-premature, non-aberrant AES (origin right-sided) recorded at the RA. Although average potential voltages decreased, several electrodes demonstrate a local increase in potential voltages. Potential morphology was comparable between SR and AES. Upper right panel: One SR beat and a moderate premature AES with mild/opposite aberrancy (origin left-sided) recorded at BB. Compared with SR, the AES resulted in a decrease of potential voltages and an increase in the number of SDPs, LDPs and FPs. Lower left panel: One SR beat and a moderate premature AES with severe aberrancy (origin left-sided) recorded at the PVA. There was a large spatial variability in potential voltage differences between SR and the AES. Compared to SR, there was a specific increase in the number of LDPs and fractionation duration. Lower right panel: One SR beat and a mild premature AES with mild/opposite aberrancy (origin left-sided) recorded at the LA. Compared with SR, there was a large decrease in potential voltages and number of SPs. There was a large increase in the number of SDPs, LDPs and FPs, with severe prolongation of FPs. AES, atrial extrasystole; AF, atrial fibrillation; BB, Bachmann's bundle; CABG, coronary artery bypass grafting; FD, fractionation duration; FP, fractionated potentials; MVD, mitral valve disease; LA, left atrium; LDP, long double potentials; LVA, low-voltage area; PI, prematurity index; PVA, pulmonary vein area; RA, right atrium; SDP, short double potentials; SP, single potentials; SR, sinus rhythm.

were computed, including potential voltages and fractionation. The potential voltage was defined as the peak-to-peak amplitude of the steepest deflection; potentials with an amplitude below 1.0 mV were defined as low voltage.[10] The proportion of low-voltage potentials was used as quantification of the amount of low-voltage areas (LVAs).

Potentials were classified as single- (SP, single negative deflection), short double- (SDP, interval between deflections <15 ms), long double- (LDP, deflection interval ≥15 ms), or fractionated potentials (FP, ≥ 3 deflections), as illustrated in Supplementary material online, *Figure S1*. The time difference (ms) between the first and last deflection of double potentials (DP; SDP + LDP) and FPs is defined as fractionation duration (FD). Areas of simultaneous activation were excluded from analysis in order to avoid inclusion of far-field potentials. For all electrophysiological parameters the median of the preceding sinus beats was taken and compared to the median of the AES. The difference was considered as the effect provoked by AES.

Classification of atrial extrasystoles

AES were defined as beats with either a shortening in cycle length of ≥25% compared to the previous sinus beat measured at the same mapping site and/or an aberrant activation pattern compared to the SR beats.[6] The degree of prematurity (prematurity index) was determined for beats preceded by at least two sinus beats, as:

$$\mathrm{PI} = \frac{\mathrm{CL_{SR}} - \mathrm{CL_{AES}}}{\mathrm{CL_{SR}}} \cdot 100\%,$$

with $\mathrm{CL_{AES}}$ equals the cycle length of the spontaneous AES and $\mathrm{CL_{SR}}$ the cycle length of the preceding two sinus beats. Premature AES were categorized into three groups based on their prematurity as mild (25 < PI < 35%), moderate (35 < PI < 50%) and severe (PI > 50%). The degree of aberrancy was determined by estimating the local propagation angle relying on fitting polynomial surfaces, as described before.[11] Aberrancy was categorized according to the shift in direction of the local wavefront trajectory ($\measuredangle$) as: none ($|\measuredangle| < 22.5^\circ$), mild/opposite ($|\measuredangle| > 157.5^\circ$), moderate ($22.5 \leq |\measuredangle| < 67.5^\circ$ or $112.5 < |\measuredangle| \leq 157.5^\circ$) and severe/perpendicular ($67.5 \leq |\measuredangle| \leq 112.5^\circ$). As AES emerging as an epicardial breakthrough spread in multiple directions, the degree of aberrancy could not be determined and therefore these AES were excluded from analyses.

Statistical analysis

Normally distributed data are expressed as mean ± SD, whereas skewed data are expressed as median [25th–75th percentile]. Clinical characteristics were compared using Student's *T*-test or Mann–Whitney *U* test when appropriate. Categorical data are expressed as number (percentage) and analyzed with a $\chi 2$ or Fisher exact test.

To analyze the difference between SR and AES, a paired *T*-test or Wilcoxon signed-rank test was used. The differences were presented as mean [95% CI]. Correlation was determined by ordinary least squares regression. A *P*-value <0.05 was considered statistically significant. A Bonferroni correction was applied when appropriate.

Results

Study population

Clinical characteristics of the study population [*N* = 287, 198 male (69%), age 68 ± 10 years] are summarized in Supplementary material online, *Table S1*. Patients underwent either CABG (IHD: *N* = 133; 46%), aortic valve surgery with or without CABG [(i)AVD: *N* = 80; 28%] or mitral valve surgery with or without CABG [(i)MVD: *N* = 74; 26%]. Sixty patients (21%) had a history of AF including paroxysmal (*N* = 40; 67%), persistent (*N* = 18; 30%) and longstanding persistent AF (*N* = 2; 3%).

Characteristics of AES

In total, 837 unique AES were included for analysis (2 [1–4] AES per patient). Most AES were recorded at the RA (*N* = 355, 42%) followed by LA (*N* = 186, 22%), PVA (*N* = 149, 18%) and BB (*N* = 147, 18%). Average $\mathrm{CL_{SR}}$ was 842 ± 191 ms, while average $\mathrm{CL_{AES}}$ was 592 ± 202 ms resulting in an average prematurity index of 28% [12–45]. A total of 457 (55%) AES were classified as premature. Of all AES, 581 (69%) were recorded in patients without AF. On average, 2 [1–4] PACs per patient were included in both the no AF and AF group (*P* = 0.393).

Figure 1 illustrates four typical examples of LAT maps and unipolar potentials during SR and corresponding AES during different degrees of prematurity and aberrancy. In all recordings, spontaneous AES resulted in clear changes in either potential voltages or potential type morphologies. Remarkably, within the recording area, there was a large spatial variation in effect provoked by the AES; e.g. (i) potential voltages either increased or decreased; (ii) fractionation either arose or disappeared; and (iii) FD of fractionated potentials either increased or decreased.

Effect of prematurity on potential morphology

Only weak or moderate correlations were found between EGM morphology parameters and prematurity indices of all AES (R^2 < 0.299, *P* < 0.001). All premature AES were further subdivided into four classes according to their prematurity as non- (*N* = 380), mild (*N* = 117), moderate (*N* = 184) and severe (*N* = 156) premature AES. Electrophysiological characteristics of potentials within each of these classes are listed in Supplementary material online, *Table S2* and visualized in *Figure 2*. Although there were only weak correlations between EGM morphology parameters and prematurity indices, there was a larger decrease in average potential voltage and number of SPs, as well as a larger increase in the number of LVAs, SDPs, LDPs, and FPs (*P* < 0.015) during severe premature AES compared to non-premature AES. There was no effect of prematurity on FD of both DP and FP.

There were considerable regional differences in the effect of prematurity on potential voltages and fractionation. At the RA, potential voltages and the number of SPs decreased and the number of SDPs increased with increasing severity of prematurity (*P* < 0.001), while at BB only potential voltages decreased considerably during severe premature AES. At all other sites, no clear relations were found between various EGM morphology parameters and prematurity.

Effect of aberrancy on potential morphology

All 837 AES were categorized according to the mean shift in direction of the propagating wavefront as non- (*N* = 270), mild/opposite (*N* = 58), moderate (*N* = 355), and severe (*N* = 154) aberrant. Directional effects of AES on potential morphology characteristics are listed in Supplementary material online, *Table S3* and illustrated in *Figure 3*. Although potential voltages decreased during all aberrant AES, the largest decrease was found in mild/opposite and severe aberrant AES (−1.6 [−2.2, −1.1] mV and −1.7 [−2.0, −1.4] mV, respectively, *P* < 0.001). In all aberrancy categories, the number of SPs decreased compared to non-aberrant AES (*P* < 0.001).

There were significant interregional differences in the impact of aberrant AES on potential morphology characteristics. At the RA, the most prominent effect of aberrancy was caused by severe aberrant AES, consisting of a decrease in potential voltages and number of SPs, and an increase in the number of SDPs (*P* < 0.001 for each). Moderate aberrant AES resulted only in an increase in the number of SDPs (*P* < 0.001). At BB, only mild/opposite AES resulted in a decrease in potential voltages (*P* = 0.009), whereas at the LA, both mild/opposite and severe aberrant AES provoked the largest differences in potential morphology characteristics. This consisted of a decrease in potential voltages and number of SPs, as well as an increase in the amount of

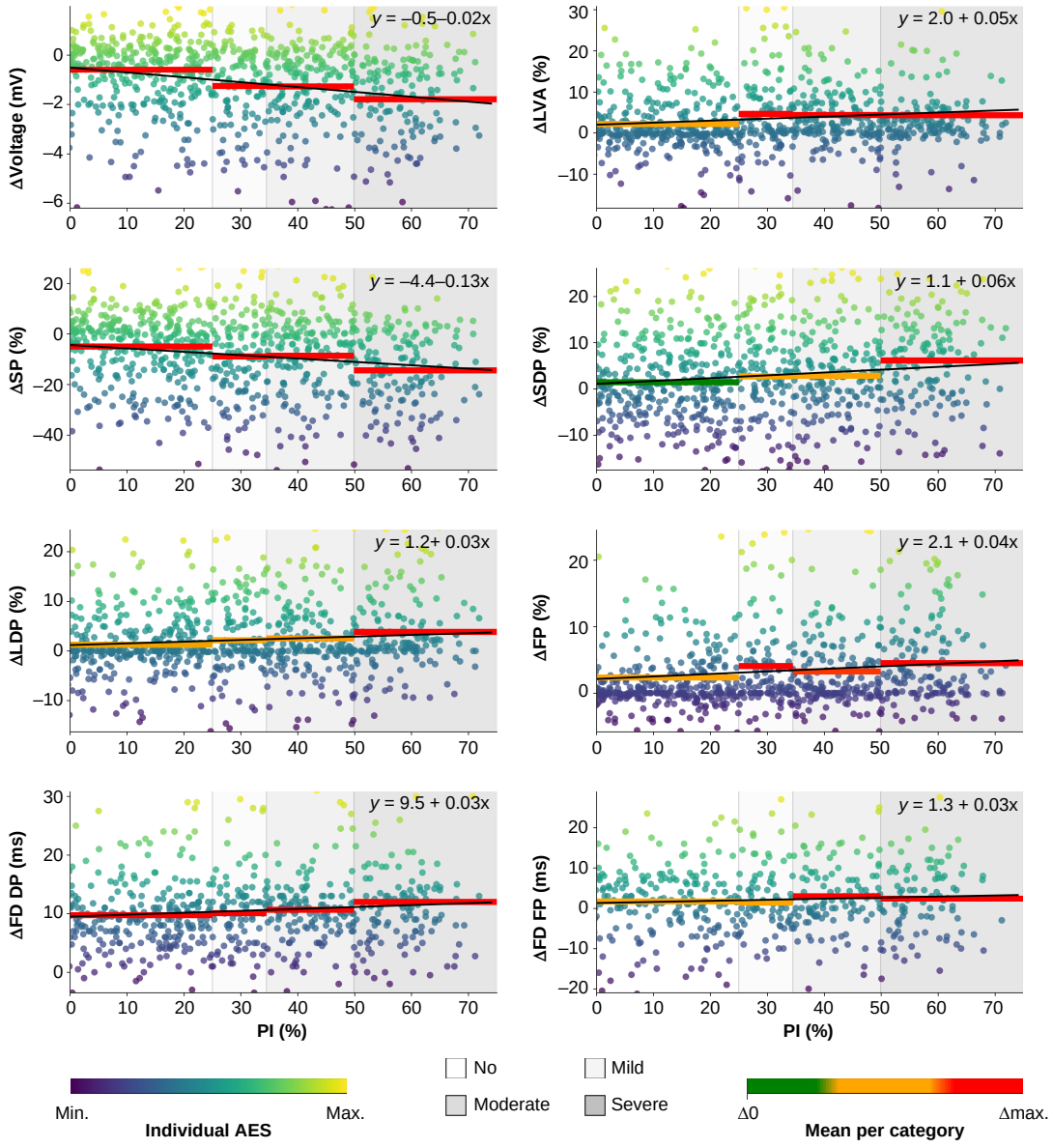

Figure 2 Relation between prematurity index and potential characteristics. In each panel, prematurity indices are plotted against each of the EGM parameters. Each individual AES is indicated by a dot of which colour indicates the average provoked effect. The colour scale ranges from the smallest to the largest effect of all AES. The black line indicates the linear correlation between prematurity index and the effect provoked by all AES. Four (none, mild, moderate, severe) prematurity classes are separately highlighted by a grayscale, ranging from light grey to dark grey, respectively. The average for each class is coloured according to the mean effect, ranging from 0 to the maximum difference of all classes. AES, atrial extrasystole; DP, short + long double potentials; FD, fractionation duration; FP, fractionated potentials; LDP, long double potentials; LVA, low-voltage area; SDP, short double potentials; SP, single potentials.

LDPs and FPs ($P \leq 0.001$ for each). At the PVA, only severe aberrant AES resulted in a significant increase in the number of FPs ($P = 0.004$). There were no regional differences between the degree of aberrancy and FD of both DPs and FPs.

Interplay of prematurity and aberrancy

Figure 4 shows the mean effect of AES with various degrees of prematurity and aberrancy combined on the various EGM morphology characteristics. As can be seen, all EGM morphology parameters are most severely affected by either mild/opposite or severe aberrant AES, independently of the degree of prematurity. The smallest effect had, not surprisingly, non-premature AES with a comparable direction of activation as during SR.

Influence of atrial fibrillation episodes

As the effect of mild/opposite and severe aberrant AES was most prominent, these types of AES were further compared between patients with and without AF. In total, 147 AES were recorded in patients without AF and 65 in patients with AF. As listed in *Table 1*, there was a more prominent effect of AES on EGM morphology parameters in

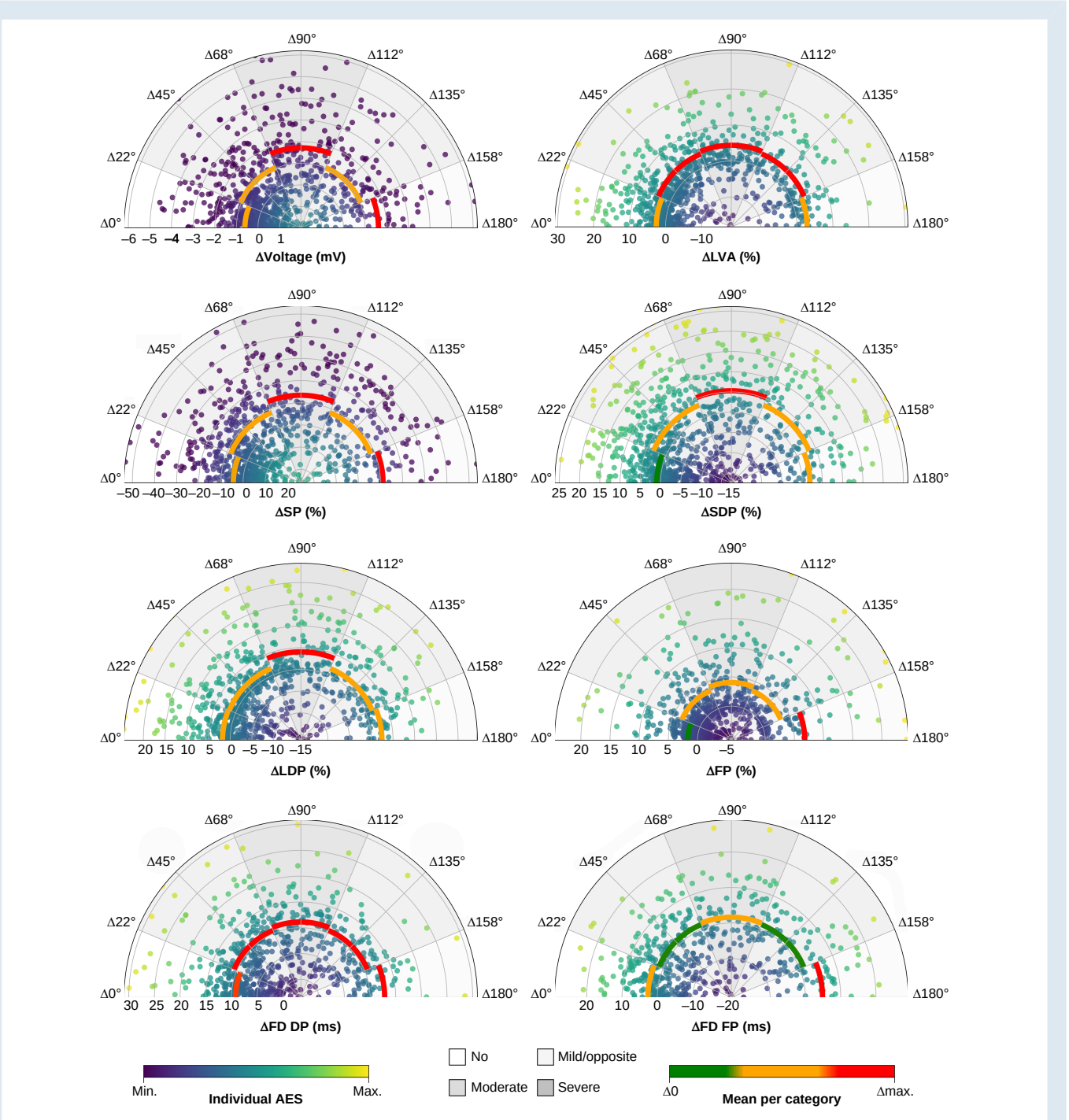

Figure 3 Relation between aberrancy and potential characteristics. In each panel, the absolute difference in propagation direction for each AES is plotted against the various EGM parameters in polar plots. Each individual AES is indicated by a dot of which colour indicates the average provoked effect. The colour scale ranges from the smallest to the largest effect of all AES. Four (none, mild/opposite, moderate, severe) aberrancy classes are separately highlighted by a grayscale, ranging from light grey to dark grey, respectively. The average for each class is coloured according to the mean effect ranging from 0 to the maximum difference of all classes. AES, atrial extrasystole; DP, short + long double potentials; FD, fractionation duration; FP, fractionated potentials; LDP, long double potentials; LVA, low-voltage area; SDP, short double potentials; SP, single potentials.

patients with AF; SPs changed more often to FPs during AES as compared with patients without AF (74% vs. 83% of the AES; 4.7 [1.8–9.6] % vs. 7.2 [4.1–12.0] %, $P = 0.007$). Comparing the effects of AES for each atrial region separately, clear differences between patients with and without AF were only found at the RA. At this site, potential voltages were lower in patients with AF (no AF: −1.2 [−1.7, −0.7] mV vs. AF: −2.8 [−3.5, −2.1] mV, $P < 0.001$). In addition, the number of SPs was lower (no AF: −8.9 [−13.5, −4.4] % vs. AF: −25.6 [−34.7, −16.5] %, $P = 0.002$) as there were more SDPs (no AF: + 4.6 [2.1, 7.1] % vs. AF: + 13.5 [8.4, 18.5] %, $P = 0.003$) and FPs (no AF: + 2.1 [0.5, 3.7] % vs. AF: +

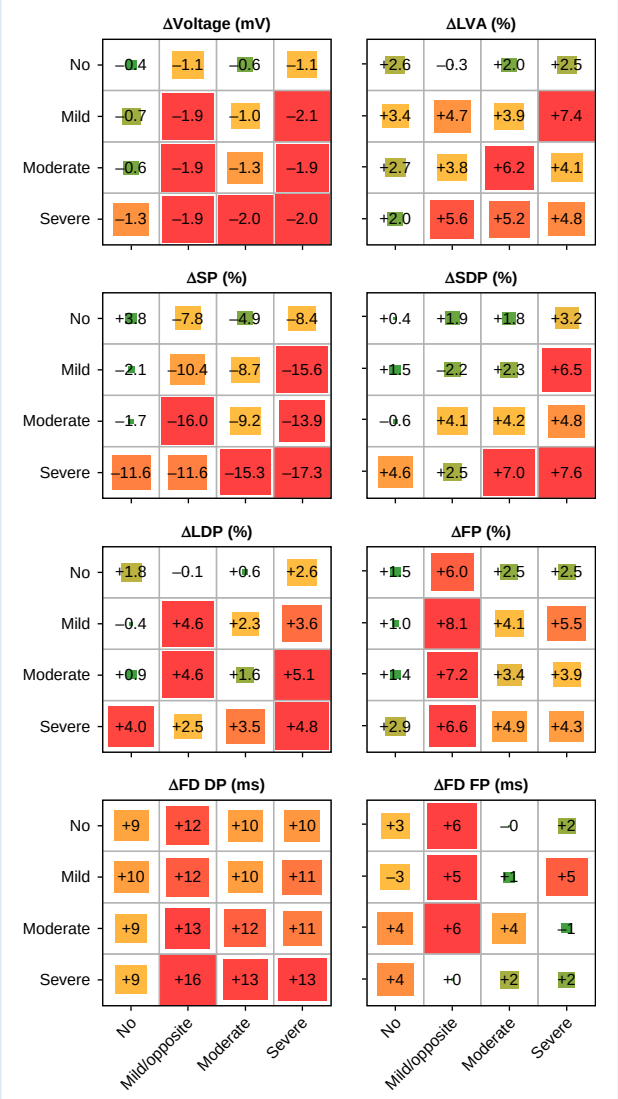

Figure 4 Interrelationship between aberrancy and prematurity. The mean effect of each parameter is visualized for all AES with varying degrees of aberrancy (*x*-axis) and prematurity (*y*-axis). The size and colour (from green to red) of the squares represent the mean effect provoked by the AES in each class. DP, short + long double potentials; FD, fractionation duration; FP, fractionated potentials; LDP, long double potentials; LVA, low-voltage area; SDP, short double potentials; SP, single potentials.

6.6 [2.8, 10.4] %, $P = 0.030$). There was a trend towards a higher number of FPs in patients with AF at BB (no AF: + 2.1 [−0.7, 5.0] % vs. AF: + 9.3 [1.8, 16.8] %, $P = 0.058$), while no clear differences were found at the PVA and LA between patients with and without AF.

Discussion

This is the first study reporting on the impact of spontaneous AES and SR on EGM morphology. The degree of aberrancy and not the degree of prematurity had the most prominent effect on EGM morphology, including potential voltage and fractionation. Mild/opposite and severe aberrant AES caused the largest decrease in potential voltages and increase in fractionation. In patients with AF there was a considerable decrease in potential voltages and increase in fractionation caused by spontaneous AES compared to patients without AF particularly at the RA. These observations indicate enhanced direction-dependency of intra-atrial conduction in patients with AF.

Arrhythmogenic effect of AES

Spontaneous AES are often referred as benign interruptions of SR, although AES are known to trigger episodes of AF, as in more than 90% of the AF cases episodes are preceded by an AES.[12,13] While the majority of AES triggering AF originate from within the PVs, AES emerging from, e.g. the superior vena cava, LA posterior free wall, LA appendage, terminal crest and interatrial septum also play an important role.[4] It is therefore not surprising that isolation of the PVs alone is not always successful to prevent initiation of AF episodes. In clinical practice, mapping of AES is often limited to identification of its origin by identifying the earliest activation site relative to the fixed timing reference rather than studying its mechanistic (electrical) effects on the atrial tissue. This is mainly due to technical challenges as the number of simultaneous recording electrodes is limited during endovascular mapping procedures. Consequently, little is known about the ultimate determinant factors of AF initiation by spontaneous AES. However, novel approaches, such as the dual-reference approach, might enable more extensive research on electrophysiological characteristics of frequent spontaneous AES in the near future.[14] Mechanistic insights of spontaneous AES are therefore mainly limited to intra-operative (endo-)epicardial mapping procedures in patients with structural heart disease.

(Non-uniform) anisotropic conduction

Atrial tissue is considered to be anisotropic, implying that electrical conduction is much faster along the longitudinal direction of myocardial fibers than in transverse direction.[1] Within the atria, there are specific regions of preferential conduction, e.g. terminal crest and BB, which appear to be optimized for fast excitation of atrial tissue.[15] However, altered cell-to-cell communication and tissue damage can result in a discontinuous distribution of conduction properties. This is known as non-uniform anisotropy. These changes in anisotropic properties of cardiomyocytes can be pro-arrhythmogenic as they may cause unidirectional block and reentry. It is likely that the magnitude of changes in tissue anisotropy depends on the location within the atria, caused by, i.e. tissue thickness, fiber orientation, local tissue damage and underlying heart disease. In addition, as conduction disorders are direction and frequency dependent, electrophysiological properties indicating non-uniform anisotropy can be 'hidden' during normal SR. In these areas, potential fractionation can occur, caused by asynchronous activation of groups of cardiomyocytes that are separated by areas in which there is diminished or no cell-to-cell coupling.[5] Starreveld[16] presented the first human case illustrating EGM morphological manifestations of direction- and rate-dependent anisotropic conduction in a 76-year-old patient with long-standing persistent AF, resulting in low-amplitude, fractionated unipolar potentials. In this study, we now demonstrated in a large population of patients with and without a history of AF that spontaneous AES are characterized by a clear increase of potential fractionation and a decrease of potential voltages, which depended particularly on the degree of aberrancy. This indicates the presence of irregular discontinuous propagation by anisotropic structural discontinuities that could be proarrhythmic, even in patients without prior AF episodes. These areas, however, were more pronounced in AF patients, indicating a higher degree of tissue remodeling compared to patients without AF. This finding could explain the higher vulnerability to AES in triggering AF in patients with spontaneous AF episodes.

Rate- and direction dependency

Anisotropy is not only determined by structural determinants such as cell size and shape, myocardial fibrosis and gap junction distribution, but it can

Table 1 Influence of AF episodes in mild/opposite and severe aberrant AES

	Δ(AES-SR) without AF	Δ(AES-SR) with AF	*P*-value
Voltage (mV)			
All beats	−1.6 [−1.9, −1.3]	−1.9 [−2.3, −1.4]	0.179
RA	−1.2 [−1.7, −0.7]	−2.8 [−3.5, −2.1]	<0.001
BB	−1.5 [−1.8, −1.1]	−1.3 [−1.7, −0.9]	0.301
PVA	−1.5 [−2.3, −0.7]	−1.0 [−1.9, −0.0]	0.193
LA	−2.8 [−3.7, −1.9]	−2.3 [−3.5, −1.0]	0.181
LVA (%)			
All beats	+3.8 [2.3, 5.4]	+4.3 [1.6, 6.9]	0.114
RA	+3.1 [1.0, 5.1]	+5.8 [2.6, 9.0]	0.103
BB	+5.3 [2.0, 8.7]	+8.6 [0.8, 16.5]	0.493
PVA	+3.6 [−0.7, 7.9]	−0.1 [−6.5, 6.3]	0.466
LA	+4.7 [0.6, 8.9]	+4.5 [2.2, 6.8]	0.123
SP (%)			
All beats	−10.6 [−13.7, −7.6]	−17.6 [−22.8, −12.4]	0.014
RA	−8.9 [−13.5, −4.4]	−25.6 [−34.7, −16.5]	0.002
BB	−9.2 [−14.5, −4.0]	−15.1 [−23.9, −6.4]	0.121
PVA	−11.3 [−20.7, −1.8]	−9.2 [−20.9, 2.6]	0.308
LA	−15.4 [−21.1, −9.7]	−20.6 [−29.9, −11.2]	0.200
SDP (%)			
All beats	+3.5 [1.8, 5.3]	+6.2 [3.3, 9.2]	0.153
RA	+4.6 [2.1, 7.1]	+13.5 [8.4, 18.5]	0.003
BB	+3.0 [−1.0, 7.1]	+4.7 [−1.0, 10.4]	0.353
PVA	−0.2 [−5.8, 5.5]	+2.2 [−2.4, 6.9]	0.325
LA	+4.3 [1.4, 7.2]	+4.1 [−2.5, 10.7]	0.250
LDP (%)			
All beats	+3.7 [2.1, 5.2]	+3.4 [1.0, 5.9]	0.398
RA	+2.2 [0.1, 4.3]	+5.5 [1.7, 9.2]	0.110
BB	+4.0 [1.3, 6.8]	+1.2 [−2.0, 4.4]	0.063
PVA	+7.0 [1.0, 13.0]	+0.8 [−5.5, 7.2]	0.087
LA	+4.4 [2.0, 6.8]	+5.9 [2.1, 9.8]	0.425
FP (%)			
All beats	+3.4 [2.2, 4.6]	+7.9 [5.2, 10.7]	0.002
RA	+2.1 [0.5, 3.7]	+6.6 [2.8, 10.4]	0.030
BB	+2.1 [−0.7, 5.0]	+9.3 [1.8, 16.8]	0.058
PVA	+4.4 [1.6, 7.3]	+6.1 [0.3, 11.9]	0.343
LA	+6.8 [3.8, 9.7]	+10.5 [5.2, 15.9]	0.168
FD DP (ms)			
All beats	+11.4 [10.4, 12.5]	+12.0 [9.9, 14.0]	0.079
RA	+11.5 [9.8, 13.2]	+10.4 [8.3, 12.6]	0.295
BB	+10.5 [7.3, 13.7]	+8.4 [6.4, 10.3]	0.091
PVA	+12.5 [11.4, 13.6]	+10.7 [8.1, 13.4]	0.010
LA	+11.4 [9.8, 13.1]	+18.6 [12.0, 25.3]	0.047
FD FP (ms)			
All beats	+1.6 [−1.0, 4.2]	+4.6 [2.1, 7.1]	0.276
RA	−0.7 [−5.2, 3.7]	+3.1 [−0.2, 6.5]	0.179
BB	−0.0 [−3.7, 3.6]	+0.2 [−3.4, 3.9]	0.478
PVA	+0.8 [−4.4, 6.0]	+4.5 [−0.5, 9.5]	0.279
LA	+7.8 [1.4, 14.1]	+11.0 [4.7, 17.2]	0.326

Values are presented as median [25th–75th percentile] or as mean [95% CI].
AES, atrial extrasystole; AF, atrial fibrillation; BB, Bachmann's bundle; DP, short + long double potentials; FD, fractionation duration; FP, fractionated potentials; LA, left atrium; LDP, long double potentials; LVA, low-voltage area; PVA, pulmonary vein area; RA, right atrium; SDP, short double potentials; SP, single potentials; SR, sinus rhythm.

also be influenced by functional contributors.[15] Spach *et al.* demonstrated anisotropy to be rate- and direction dependent, as higher pacing rates resulted in lower transverse conduction velocity in relation to longitudinal conduction velocity, and premature electrical stimulation in non-uniform but not in uniform anisotropic tissue resulted in unidirectional longitudinal conduction block or a dissociated type of zigzag longitudinal conduction.[17,18] Consistent with these studies, we also observed more low-voltage fractionated potentials during spontaneous AES. Also, we demonstrated that in a significant part of the AES, smooth and biphasic extracellular potentials transformed into fractionated potentials, particularly in AF patients. These observed fractionated potentials reveal the enhanced non-uniformity of anisotropic tissue in AF patients. Although in our study there was no clear relation between the change in electrophysiological parameters and prematurity, lower potential voltages and more fractionation were found in the most severe premature AES. Several studies also showed that more severe premature AES provoke more conduction block, slower conduction and more local directional heterogeneity in conduction velocity vectors compared to non/mild-premature AES.[6,19] However, as AES near the refractory period are more likely to initiate AF episodes, it is expected that AES near the refractory period will result in even more severe alterations in unipolar potential morphology.[20,21]

As demonstrated in our current study, AES with severe aberrancy result in the most severe changes in unipolar voltage and potential morphology. However, we also demonstrated that AES with a wavefront direction opposite to the wavefront direction during SR frequently presented with similar alterations as compared with the severe aberrant AES. While Teuwen *et al.*[6] and Van der Does *et al.*[22] only demonstrated a severe increase in conduction block and endo-epicardial asynchrony during severe aberrant AES, they did not find similar results during mild/opposite aberrant AES. We also demonstrated significant regional differences in effect of aberrancy. It is therefore likely that the condition of the underlying tissue predominantly determines the effect of either prematurity or aberrancy. Since the largest effect provoked by AES is achieved by any change in wavefront direction, in theory, any premature aberrant AES originating not from the sino-atrial node area may result in severe conduction disorders in non-uniform anisotropic tissue, thereby facilitating initiation of AF.

Clinical implications

In the current study, we demonstrated that spontaneous AES are particularly directional-dependent, with a more prominent effect of these AES in patients with history of AF. Hence, a significant part of conduction disorders would be missed when performing electrophysiological examination during sinus rhythm alone. As these direction-dependent conduction disorders were particularly found at the RA in patients with AF, one could consider more extensive substrate identification

by using multisite pacing and focusing on unipolar EGM characteristics. However, whether additional ablation strategies targeting these regions truly helps improving ablation outcomes needs to be examined in future studies.

Limitations

Atrial tachyarrhythmias were not initiated by the AES in this study. Although the prematurity index was relatively high in some AES, the CL_{AES} was frequently still above the expected refractory period.[20,21] Therefore, AES with more shortening of the cycle length are expected to result in a more pronounced effect. The arrhythmogenic effect of AES could only be studied at one single mapping site and not at multiple atrial regions simultaneously. Consequently, the origin of each AES and the effect on multiple atrial sites simultaneously remain unknown.

Conclusion

Spontaneous AES with an opposite or perpendicular wavefront direction to SR provoked the largest changes in unipolar potential morphology, independently of the degree of prematurity. Therefore, unipolar EGM characteristics during spontaneous AES are mainly directional-dependent and not rate-dependent. As AF patients have more severe direction-dependent conduction disorders, enhanced non-uniform anisotropy probably explains the higher vulnerability to trigger episodes of AF.

Translational perspective

This is the first study reporting on the impact of spontaneous AES on EGM morphology. We demonstrated that the degree of aberrancy and not the degree of prematurity had the most prominent effect on EGM morphology, including potential voltage and fractionation. In patients with AF there was a considerable decrease in potential voltages and increase in fractionation caused by spontaneous AES compared to patients without AF, particularly at the RA, indicating enhanced direction-dependency of intra-atrial conduction in patients with AF. Enhanced non-uniform anisotropy in these patients probably explains the higher vulnerability to trigger episodes of AF. In addition, as spontaneous AES are particularly directional-dependent, a significant part of conduction disorders would be missed when performing electrophysiological examination during sinus rhythm alone. One could therefore consider more extensive substrate identification by using multisite pacing and focusing on unipolar EGM characteristics. Future studies should examine whether additional ablation strategies targeting these regions truly help improving ablation outcomes.

Supplementary material

Supplementary material is available at Europace online.

Acknowledgements

The authors would like to kindly thank J.A. Bekkers, MD, PhD; C. Kik, MD: W.J. van Leeuwen, MD; F.B.S. Oei, MD, PhD; P.C. van de Woestijne, MD; A. Yaksh, MD, PhD; E.A.H. Lanters, MD, PhD; C.P. Teuwen, MD, PhD; E.M.J.P. Mouws, MD, PhD; J.M.E. van der Does, MD, PhD; C.A. Houck, MD, PhD; R. Starreveld, PhD; C.S. Serban, DVM; L.N. van Staveren, MD; A. Heida, MD; W.F.B. van der Does, MD; M.C. Roos-Serote, PhD; for their contribution to this work.

Funding

N.M.S.d.G., MD, PhD is supported by funding grants from NWO-Vidi (NWO-Vidi is granted via Nederlandse Organisatie voor Wetenschappelijk Onderzoek/Dutch Research Council) [grant number 91717339], Biosense Webster USA [ICD 783454] and Medical Delta.

Conflict of interest: None declared.

Data availability

The data underlying this article will be shared on reasonable request to the corresponding author.

References

1. Kléber AG, Rudy Y. Basic mechanisms of cardiac impulse propagation and associated arrhythmias. *Physiol Rev* 2004;**84**:431–88.
2. Spach MS, Dolber PC. Relating extracellular potentials and their derivatives to anisotropic propagation at a microscopic level in human cardiac muscle. Evidence for electrical uncoupling of side-to-side fiber connections with increasing age. *Circ Res* 1986;**58**:356–71.
3. Haissaguerre M, Jais P, Shah DC, Takahashi A, Hocini M, Quiniou G *et al.* Spontaneous initiation of atrial fibrillation by ectopic beats originating in the pulmonary veins. *N Engl J Med* 1998;**339**:659–66.
4. Kawai S, Mukai Y, Inoue S, Yakabe D, Nagaoka K, Sakamoto K *et al.* Non-pulmonary vein triggers of atrial fibrillation are likely to arise from low-voltage areas in the left atrium. *Sci Rep* 2019;**9**:12271.
5. Spach MS. Anisotropy of cardiac tissue: a major determinant of conduction? *J Cardiovasc Electrophysiol* 1999;**10**:887–90.
6. Teuwen CP, Kik C, van der Does L, Lanters EAH, Knops P, Mouws E *et al.* Quantification of the arrhythmogenic effects of spontaneous atrial extrasystole using high-resolution epicardial mapping. *Circ Arrhythm Electrophysiol* 2018;**11**:e005745.
7. Lanters EA, van Marion DM, Kik C, Steen H, Bogers AJ, Allessie MA *et al.* HALT & REVERSE: Hsf1 activators lower cardiomyocyt damage; towards a novel approach to REVERSE atrial fibrillation. *J Transl Med* 2015;**13**:347.
8. van der Does LJ, Yaksh A, Kik C, Knops P, Lanters EA, Teuwen CP *et al.* QUest for the arrhythmogenic substrate of atrial fibRillation in patients undergoing cardiac surgery (QUASAR study): rationale and design. *J Cardiovasc Transl Res* 2016;**9**:194–201.
9. Kik C, Mouws E, Bogers A, de Groot NMS. Intra-operative mapping of the atria: the first step towards individualization of atrial fibrillation therapy? *Expert Rev Cardiovasc Ther* 2017;**15**:537–45.
10. van Schie MS, Starreveld R, Bogers A, de Groot NMS. Sinus rhythm voltage fingerprinting in patients with mitral valve disease using a high-density epicardial mapping approach. *Europace* 2021;**23**:469–78.
11. van Schie MS, Heida A, Taverne Y, Bogers A, de Groot NMS. Identification of local atrial conduction heterogeneities using high-density conduction velocity estimation. *Europace* 2021;**23**:1815–25.
12. Johnson LS, Juhlin T, Juul-Moller S, Hedblad B, Nilsson PM, Engstrom G. A prospective study of supraventricular activity and incidence of atrial fibrillation. *Heart Rhythm* 2015;**12**:1898–904.
13. Vincenti A, Brambilla R, Fumagalli MG, Merola R, Pedretti S. Onset mechanism of paroxysmal atrial fibrillation detected by ambulatory Holter monitoring. *Europace* 2006;**8**:204–10.
14. Chen M, Yang M, Li W, Zhang PP, Zhang R, Mo BF *et al.* Novel dual-reference approach facilitates the activation mapping and catheter ablation of premature atrial complexes with non-pulmonary vein and non-superior vena cava origins. *Europace* 2023;**25**:146.
15. Kotadia I, Whitaker J, Roney C, Niederer S, O'Neill M, Bishop M *et al.* Anisotropic cardiac conduction. *Arrhythm Electrophysiol Rev* 2020;**9**:202–10.
16. Starreveld R, de Groot NMS. Direction- and rate-dependent fractionation during atrial fibrillation persistence: unmasking cardiac anisotropy? *J Cardiovasc Electrophysiol* 2020;**31**:2206–9.
17. Spach MS, Kootsey JM, Sloan JD. Active modulation of electrical coupling between cardiac cells of the dog. A mechanism for transient and steady state variations in conduction velocity. *Circ Res* 1982;**51**:347–62.
18. Spach MS, Dolber PC, Heidlage JF. Influence of the passive anisotropic properties on directional differences in propagation following modification of the sodium conductance in human atrial muscle. A model of reentry based on anisotropic discontinuous propagation. *Circ Res* 1988;**62**:811–32.
19. van Schie MS, Misier NLR, Razavi Ebrahimi P, Heida A, Kharbanda RK, Taverne Y *et al.* Premature atrial contractions promote local directional heterogeneities in conduction velocity vectors. *Europace* 2023;**25**:1162–71.
20. Schmitt C, Ndrepepa G, Weber S, Schmieder S, Weyerbrock S, Schneider M *et al.* Biatrial multisite mapping of atrial premature complexes triggering onset of atrial fibrillation. *Am J Cardiol* 2002;**89**:1381–7.
21. Kawai S, Mukai Y, Inoue S, Yakabe D, Nagaoka K, Sakamoto K *et al.* Location and coupling interval of an ectopic excitation determine the initiation of atrial fibrillation from the pulmonary veins. *J Cardiovasc Electrophysiol* 2022;**33**:629–37.
22. van der Does L, Kharbanda RK, Teuwen CP, Knops P, Kik C, Bogers A *et al.* Atrial ectopy increases asynchronous activation of the endo- and epicardium at the right atrium. *J Clin Med* 2020;**9**:558.